LONG INTEGRATION FINE RESOLUTION SAR IMAGE FORMATION

TAN Ngee Leng, LEE Sze Li.

DSO National Laboratories

ABSTRACT

To perform fine resolution SAR imaging, the radar is required to image the area of interest for a long period of time. In this paper, the signal processing aspects of processing such SAR data is described. The signal processing challenges are to estimate the large motion errors contributed by the long imaging time and to limit the phase errors due to approximation in the signal modeling for fine resolution image formation. This paper presents the implementation of a sub-spot Polar Format technique with autofocus to process data collected with long integration time. The sub-spot technique developed produced sub-spot images of the radar footprint. The full SAR image is formed by mosaic the individual sub-spots. This technique allows the formation of a large scene image at fine resolution while utilizing the efficient Polar Format Algorithm (PFA).

1. INTRODUCTION

The next generation SAR will have long integration time fine resolution imaging capability (< 1ft). The fine range resolution is a function of transmission bandwidth. The hardware challenges of the wideband radar electronics are not within the scope of this paper. This paper describes the signal processing aspects of focusing long integration time fine resolution SAR imagery. To achieve azimuth resolution of approximately 1 foot would require a synthetic aperture of a few kilometers for microwave SAR imaging. Depending on the speed of the platform, integration time up to tens of seconds may be required. Such fine two-dimensional imaging places a severe demand for motion compensation. The residual errors after motion compensation should be less than 1 resolution cell.

With long integration time fine resolution SAR, the number of samples to present an image is tremendous. Therefore, it is important to develop an efficient image formation algorithm. In Spotlight SAR, the Doppler spectrum of the received SAR signal phase history is the sum of the azimuth scene bandwidth and the Doppler spectrum subtended by the coherent imaging angle required for azimuth resolution. Hence, a high PRF is usually needed if frequency domain algorithms such as ω-k and chirp scaling algorithms are used [1]. However, a high PRF is not used to avoid range ambiguities. With limited duty cycle for TWT, at high PRF, the pulse length used for transmission is decreased and the range swath that can be sampled unambiguously is reduced in range deramp processing.

In fine resolution airborne SAR system, PRF is usually chosen to ensure the Doppler spectrum due to the antenna beamwidth is sampled unambiguously, but usually less than the total bandwidth required for frequency domain algorithms. Although there are signal processing methodologies [4] to unwrap the ambiguous spectrum, the number of samples is 'artifically' upsampled to the required sampling rates which will increase the processing time.

In this paper, an image formation algorithm was developed to process SAR data with integration time of 40 seconds to achieve an azimuth resolution of 1ft. The algorithm process flow is illustrated in Figure 1.1.

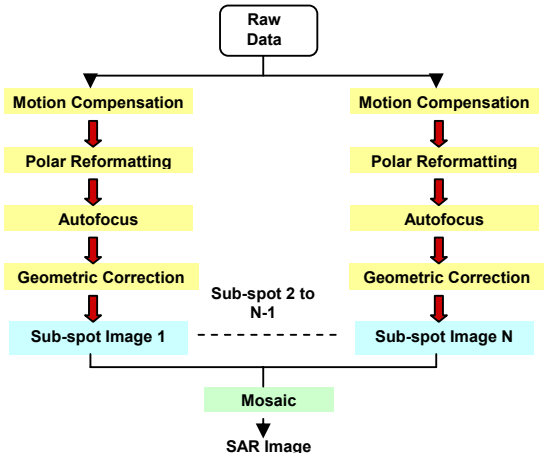

Figure 1.1: Processing flow chart of developed technique

The core of this algorithm is the sub-spot Polar Format and Autofocus. Polar Format algorithm [1,3] was selected due to its low PRF requirement as compared to frequency domain algorithms. The motion compensation process in Polar Format performs effectively a dechirp in both range and azimuth. Therefore, the PRF used need only to sample the azimuth scene size umambiguously. However, due to planar wavefront approximations made in Polar Format, the residual range curvature errors limit the scene size that be processed. A sub-spot Polar Format algorithm is developed where the entire footprint is split into several sub-spots and process separately. This configuration also eases the implementation of parallel processing.

The autofocus is the most critical module of the processing. Due to long integration time, the magnitude of the phase errors is expected to be large. A Quadratic Phase Autofocus (QPA), a variant of Phase Difference Algorithm[1] and High Order Phase Autofocus (HOPA) algorithms, were developed to estimate both low and high order phase errors effectively.

2. METHODS

A sub-spot Polar Format algorithm (refer to Fig. 1.1) is developed where the motion compensation is performed specifically to each sub-spot center as shown in Figure 2.1. A low-pass filter is then applied to obtain the scene of interest. The filtering process can be implemented together with the

0-7803-8554-3/04/$20.00 ©2004 IEEE.

interpolation process in Polar Format. To achieve the required resolution, the full aperture is still processed for each sub-spot. The phase errors largely due to motion errors are expected to be large. Therefore, the core of the image formation algorithm is the autofocus algorithm to estimate both low and higher order phase errors. Detailed analysis of the phase history of the SAR signatures indicates that images formed will be geometrically distorted. A Geometric correction of each sub-spot is needed before mosaic the individual sub-spots to produce the full image. Sub-spot images formed will be rotated by the mid-aperture incidence angles at the sub-spot centers.

In Fig. 2.1, the range $\hat{R}_{s1}, \hat{R}_{s2}$ represent the actual slant ranges from the transmit platform to the centres of sub-spot 1 and sub-spot 2 respectively. The angle θ_1, θ_2 represent the mid-aperture incidence angles at the sub-spot centers of sub-spot 1 and sub-spot 2 respectively. Sub-spot processing allows any sub-spot of interest to be selected for processing.

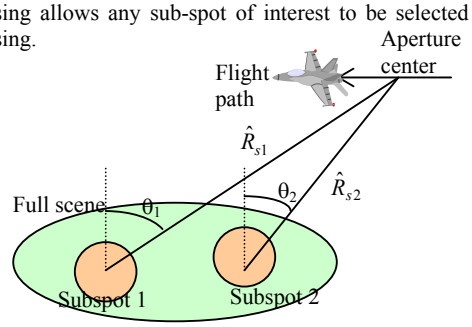

Figure 2.1: Illustration of Sub-Spot PFA image formation

2.1. Motion Compensation

The objectives of motion compensation are to ensure returns from scene centre appear at the same range gate and the chosen scene centre possesses zero Doppler or constant phase. The process is performed in two stages: (1) coarse and fine range cell migration correction (RCMC); (2) phase compensation.

The radar data collection system performs the coarse range cell migration by making real time adjustments to the radar range gate during the data collection in order to keep the desired scene within the narrow range window. Due to the quantized steps adjustment after few PRIs, discontinuity occurs. These discontinuities can be rectified by the fine RCMC process.

The fine RCMC involves determining the difference between actual slant range $\hat{R}_{sn}$ of the sub-spot centre for sub-spot n to the transmit platform and the quantized slant range $\hat{R}_q$ from the coarse RCMC. The actual slant range is derived from the GPS/INS data.

$$\Delta\hat{R}_n = \hat{R}_{sn} - \hat{R}_q \tag{2.1.1}$$

Both $\hat{R}_{sn}$ and $\hat{R}_q$ are a function of the platform position along the synthetic aperture. The number of pixels to shift for each particular range line in each sub-spot is

$$N_{pix,n} = \frac{\Delta\hat{R}_n}{c/2f_s} \tag{2.1.2}$$

where c is the speed of light and f_s is the sampling frequency. $N_{pix,n}$ is likely to be a non-integer value and therefore interpolation is required to perform fine RCMC up to sub-pixel accuracy.

The final process of motion compensation is to stabilize the phase of the sub-spot center by multiplying each synthetic PRI with the phase.

$$e^{\left(j\frac{4\pi\hat{R}_{sn}}{\lambda}\right)} \tag{2.1.3}$$

where $\hat{R}_{sn}$ is the distance from the platform to the sub-spot centre of sub-spot n.

2.2. Polar Format Algorithm

2.2.1. SAR Polar Format Signal Model

Consider the SAR imaging geometry illustrated in Figure 2.2. Let R_i be the range to target i, R_c be the range to scene center and R_s be the range to scene center at the aperture center. The symbol $\hat{a}$ and $\hat{b}$ represent the unit vectors for a and b. The scene center is denoted (0, 0). The aircraft position denoted as (a, R_s – b) and the target position as (x, y). The range from the platform to scene center can be expressed as

$$R_c = \sqrt{a^2 + (b - R_s)^2} \tag{2.2.1}$$

and platform range to other targets in the scene is

$$R_i = \sqrt{(x-a)^2 + [y - (b - R_s)]^2} \tag{2.2.2}$$

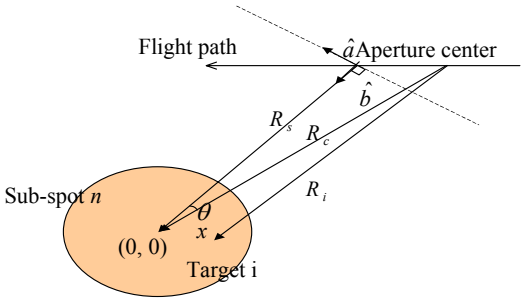

Figure 2.2: Spot Imaging Geometry

The phase history of the return signal after motion compensation is given by

$$e^{\left(j\frac{4\pi dR}{\lambda}\right)} \tag{2.2.3}$$

where dR is

$$dR = R_i - R_c$$

Expanding the expression for dR, we get

$$\exp\left\{ j\frac{4\pi}{\lambda}\left[x \cdot g_x(x,y)\cdot \sin\theta + y \cdot g_y(x,y)\cdot \cos\theta\right]\right\} \exp\left(j\phi(x,y,a,b)\right)$$

where

$$g_x(x,y) = \left[1 - \frac{y}{R_s} + ...\right] + \frac{b}{a}\left[-\frac{x^2}{2R_s} + ...\right]$$

$$g_y(x,y) = \left[1 + \frac{x^2}{2yR_s} + \mathrm{K}\right]$$

$$\phi(x,y,a,b) = \frac{4\pi}{\lambda R_c}\left\{-\frac{a^2y^2}{2R_s^2} + \frac{a^2x^2}{2R_s^2} + ...\right\} + \frac{4\pi}{\lambda R_c}\left\{-\frac{xyab}{R_s^2} + \frac{a^2bx^2}{R_s^3} + ...\right\}$$

$$\sin\theta = \frac{a}{R_c}, \qquad \cos\theta = \frac{-R_s + b}{R_c} \tag{2.2.4}$$

The constant term of $g_x(x,y)$ and $g_y(x,y)$ is desired for imaging while the phase term $\phi(x,y,a,b)$ is undesirable and it is important to quantify the magnitude of such phase errors if they are neglected during image formation. Substituting the desired terms into the expression in (2.2.4) gives

$$\begin{aligned}&\exp\left\{ j\frac{4\pi}{\lambda}\left[x.\sin\theta + y\cdot\cos\theta\right]\right\}\\ &= \exp\left\{j\left[k.\sin\theta\right]x + j\left[k.\cos\theta\right]y\right\}\\ &= \exp\left\{jk_x.x + jk_y.y\right\}\end{aligned} \tag{2.2.5}$$

where a two one-dimensional interpolation is employed to map the data from (k, θ) to (k_x, k_y) domain. This is also known as polar reformatting to format the data stored in polar region to a two-dimensional equal spacing rectangular region suitable for two-dimensional FFTs. The remapping is as follows:

$$k_x = k\sin\theta, \quad k_y = k\cos\theta \tag{2.2.6}$$

After the re-sampling, a two-dimensional Fourier Transform is performed to produce the SAR image.

2.2.2. Geometric Correction

The first order term of $g_x(x,y)$ and $g_y(x,y)$ will contribute a linear phase term in k_y and k_x. These linear variations will cause a spatial offset in the position of the scatterer without defocusing. Therefore, polar formatted images will suffer from geometrical distortion due to the planar wave front approximation. The distortion formulae for azimuth and range can be written as

$$az = x\left[1 - \frac{y}{R_s}\right]' - \frac{b}{a}\frac{x^2}{2R_s} \quad , \qquad rg = y + \frac{x^2}{2R_s} \tag{2.2.7}$$

where b/a is equal to the tangent of the squint angle. Equation (2.2.7) indicates that targets further will suffer from greater geometric distortions. The image is formed in (rg, az) coordinates that are polynomial functions of the actual target coordinates (x, y). Geometric correction is necessary to put the targets back onto their actual coordinates (x, y) on the SAR image map. To correct for the geometric distortion we resample the image pixels from (rg, az) to (x, y) coordinates. For the target with true location at (x, y), the distorted image shows it at ($x\left[1-\frac{y}{R_s}\right] - \frac{b}{a}\frac{x^2}{2R_s}$, $y + \frac{x^2}{2R_s}$). A two-dimensional re-sampling algorithm is required as the re-sampling equations are coupled in x and y. We used a simple bi-linear interpolator for the re-sampling.

2.2.3 SAR Polar Format Scene Size Limitation

The range curvature error denoted by $\exp\left(j\phi(x,y,a,b)\right)$ is quadratic in nature and will cause significant defocusing if its magnitude is not limited. Considering only dominant quadratic phase error terms, let us limit the phase error to less than π/4 radians. Approximating $R_c \approx R_s$, the polar format scene size for each sub-spot is limited to

$$x_0' \le \rho_{x'}\sqrt{\frac{2R_s}{\lambda}}, y_0' \le \rho_{x'}\sqrt{\frac{2R_s}{\lambda}} \tag{2.2.8}$$

where $\rho_{x'}$ is the azimuth resolution. x'_0 and y'_0 represents the cross range and range limit respectively.

2.3. Autofocus

In order to process Synthetic Aperture Radar (SAR) data, accurate position and velocity information is required of the radar platform. Unknown platform motions that usually are not compensated can cause image defocusing and distortion. Due to the long integration time, large motion errors are expected, as the synthetic aperture length transverse to achieve the required along-track resolution can be few kilometers. The autofocus is performed in two stages with the Quadratic Phase Autofocus (QPA) performed first to remove the bulk of the lower order phase errors followed by the Higher Order Phase Autofocus (HOPA).

2.3.1 Quadratic Phase Autofocus

Similar to the Phase Difference Algorithm [1], the QPA obtains the error estimate from the Fourier transform of a correlation function created from the sub-aperture data. The location of the correlation peak serves as a measure of relative shift between the images of the two sub-apertures. For range gates that contain targets that are closely located, the correlation function will be corrupted. The QPA will detect such range gates and reject them from the error estimation process.

2.3.2 Higher Order Phase Autofocus

HOPA is another class of algorithms which unlike QPA, is not model based and does not explicitly limit the order of the phase errors. Therefore, the HOPA is usually employed for high phase order autofocus. It also accurately estimates multicycle phase errors in SAR signal data.

Similar to the PGA [1-2], HOPA windows the strong targets after they are center shifted in each range bin. For HOPA, the width of the window is determined adaptively depending on the distortion of the targets. If the distortions are mainly caused by high order phase errors, the mainlobe of the impulse response of the targets will not be broadened as is for the case of quadratic phase errors. Instead, the sidelobe level will be raised. For HOPA, the sidelobe level is used to determine the window width so as to include the effects of the higher order phase error.

To select range gates for phase error estimation, the algorithm will detect range gates that contain ideal point like sources by measuring the stability of the phase history. The

algorithm gives higher weightings to range gates with phase history similar to that of ideal point like sources.

Figures 2.3 and 2.4 below illustrate the flow charts for QPA and HOPA respectively.

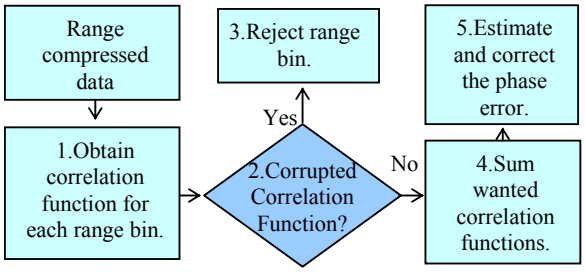

Figure 2.3: Flow chart for QPA

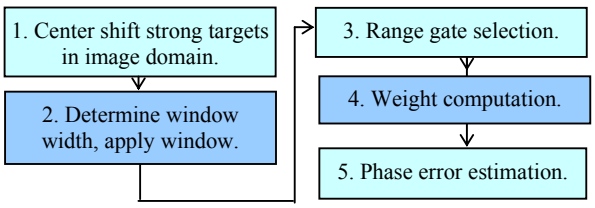

Figure 2.4: Flow chart for HOPA

3. RESULTS

The algorithm was tested using raw SAR data collected by THALES AIRBORNE SYSTEMS with coherent integration time of 40 seconds to achieve azimuth resolution down to 25cm. A trihedral corner reflector was present in the imaging site for image quality validation.

3.1 Autofocus

The autofocus results of the trihedral corner reflector (zoomed-in) are shown in Figure 3.1-3.2. The figures show that the autofocus algorithms implemented removed most of the phase errors present to give a well-focused image.

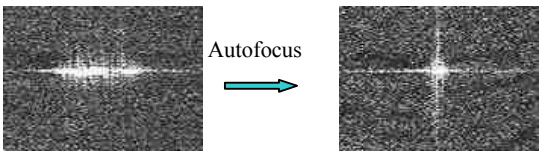

Figure 3.1: Images at 25cm resolution before and after autofocus

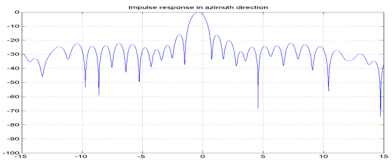

Figure 3.2

Figures 3.2 above shows the azimuth impulse response of the point target after autofocus.

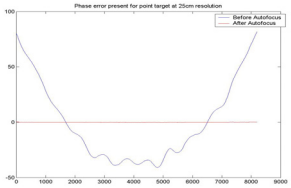

Figure 3.3: Residual phase errors before and after autofocus

Figure 3.3 illustrates the phase errors extracted before and after autofocus. The blue line clearly illustrates that the phase errors are largely quadratic in nature with sinusoidal phase errors riding on it. The red line indicates that the phase errors are largely removed after the autofocus.

Quality Metrics	Measurements
-3dB resolution (Azimuth)	25cm
PSLR (Azimuth)	-16dB

Table 1: Quality metrics measurements of focused point target

4. CONCLUSION

An improved SAR image formation algorithm was developed to produce focused fine resolution SAR imagery. The sub-spot Polar Format algorithm with autofocus was used to produce sub-spot SAR images, which are then mosaic to form the full image. The image parameters such as resolution and PSLR based on return from the trihedral corner reflector were used to validate the performance of the algorithms.

5. REFERENCES

[1] W. G. Carrara, R. S. Goodman and R. M. Majewski, eds., *Spotlight Synthetic Aperture Radar: Signal Processing Algorithms*. Boston: Artech House, 1995.

[2] D. E. Wahl, P. H. Eichel, D. C. Ghiglia, and C. V. Jakowatz, "Phase gradient autofocus – A robust tool for high resolution SAR phase correction," *IEEE Trans. Aerosp. Electron. Syst.*, vol. 30, pp. 827-834, July 1994.

[3] C. V. Jakowatz, Jr., et. al., *Spotlight-Mode Synthetic Aperture Radar: A Signal Processing Approach*, Kluwer Academic Publishers, Boston, 1996.

[4] August Golden, Jr., et. al., "Migration processing of spotlight SAR data", SPIE Vol. 2230.